J. Membrane Biol. 169, 155–165 (1999)

The Journal of
Membrane
Biology

Veratridine-Mediated Ca^{2+} Dynamics and Exocytosis in *Paramecium* Cells

M.-P. Blanchard, N. Klauke, S. Zitzmann, H. Plattner
Universität Konstanz, Fakultät für Biologie, P.O. Box 5560, D-78434 Konstanz, Germany

Received: 8 December 1998/Revised: 2 March 1999

Abstract. We analyzed $[Ca^{2+}]_i$ transients in *Paramecium* cells in response to veratridine for which we had previously established an agonist effect for trichocyst exocytosis (Erxleben & Plattner, 1994. *J. Cell Biol.* **127:**935–945; Plattner et al., 1994. *J. Membrane Biol.* **158:**197–208). Wild-type cells (7S), nondischarge strain nd9–28°C and trichocyst-free strain "trichless" (tl), respectively, displayed similar, though somewhat diverging time course and plateau values of $[Ca^{2+}]_i$ transients with moderate $[Ca^{2+}]_o$ in the culture/assay fluid (50 μM or 1 mM). In 7S cells which are representative for a normal reaction, at $[Ca^{2+}]_o$ = 30 nM (c.f. $[Ca^{2+}]_i^{rest}$ = ~50 to 100 nM), veratridine produced only a small cortical $[Ca^{2+}]_i$ transient. This increased in size and spatial distribution at $[Ca^{2+}]_o$ = 50 μM of 1 mM. Interestingly with unusually high yet nontoxic $[Ca^{2+}]_o$ = 10 mM, $[Ca^{2+}]_i$ transients were much delayed and also reduced, as is trichocyst exocytosis. We interpret our results as follows. (i) With $[Ca^{2+}]_o$ = 30 nM, the restricted residual response observed is due to Ca^{2+} mobilization from subplasmalemmal stores. (ii) With moderate $[Ca^{2+}]_o$ = 50 μM to 1 mM, the established membrane labilizing effect of veratridine may activate not only subplasmalemmal stores but also $Ca^{2+}{}_o$ influx from the medium via so far unidentified (anteriorly enriched) channels. Visibility of these phenomena is best in tl cells, where free docking sites allow for rapid Ca^{2+} spread, and least in 7S cells, whose perfectly assembled docking sites may "consume" a large part of the $[Ca^{2+}]_i$ increase. (iii) With unusually high $[Ca^{2+}]_o$, mobilization of cortical stores and/or $Ca^{2+}{}_o$ influx may be impeded by the known membrane stabilizing effect of $Ca^{2+}{}_o$ counteracting the labilizing/channel activating effect of veratridine. (iv) We show these effects to be reversible, and, hence, not to be toxic side-effects, as confirmed by retention of injected calcein. (v) Finally, Mn^{2+} entry during veratridine stimulation, documented by Fura-2 fluorescence quenching, may indicate activation of unspecific Me^{2+} channels by veratridine. Our data have some bearing on analysis of other cells, notably neurons, whose response to veratridine is of particular and continous interest.

Key words: Calcium — Exocytosis — Membrane fusion — *Paramecium* — Secretion — Veratridine

Introduction

Veratridine, like batrachotoxin and aconitine, is frequently used as a Na channel agonists [2, 21]. Yet these lipophilic alkaloids can also act rather unspecifically, e.g., by labilizing membranes (causing increased fluidity and channel activity), as shown for veratridine [2, 7, 42, 50]. Veratridine is frequently assumed to act from outside the cell, but it may also become active from inside the cell [19, 22], whereby it would have to penetrate the cell membrane [8, 22]. Activation of Na channels [1, 7, 22, 52], or possibly also of Na^+/Ca^{2+} exchangers [52] or of Ca channels [12, 51] may then ensue.

In *Paramecium*, veratridine induces trichocyst exocytosis [15, 29, 36], though less efficiently than the polyamine secretagogue, aminoethyldextrane (AED) [35, 38] or caffeine [15, 27]. For both these agents we demonstrated, also by fluorochrome analysis, the occurrence of a cortical $[Ca^{2+}]_i$ transient orginating primarily from cortical pools ("alveolar sacs" [49]) and reinforced by superimposed Ca^{2+} influx from the medium [14, 15, 26, 27]. For trichocyst secretion induced by veratridine, the source of calcium is addressed in this paper.

The strains we used were the 7S (wild type), nd9-28°C and tl. 7S cells represent the normal situation, as they possess numerous trichocysts docked at the cell membrane ready for immediate synchronous release by exocytosis. This involves membrane fusion and contents

Correspondence to: H. Plattner

discharge ("decondensation" = severalfold stretching of pear-shaped contents to needles during expulsion through exocytotic openings), [37, 38]. Membrane fusion requires a subplasmalemmal $[Ca^{2+}]_i$ increase [14, 15, 26, 27], while decondensation of contents, with no Ca detectable by x-ray microanalysis [45], requires access of Ca^{2+} to the secretory materials [5]. This normally occurs by influx of Ca_o^{2+} after formation of an exocytotic pore [37, 38]. The nd9 mutant we used was grown at a nonpermissive temperature of 28°C, so it cannot secrete any of its trichocysts, although they are docked in great numbers at the cell membrane [3, 4, 30, 40]. Their trichocyst contents can decondense in vitro, but since nd9–28°C cells cannot form an exocytotic fusion pore, Ca^{2+} must artifically obtain access to trichocyst contents to provoke their ("internal") decondensation [40]. The tl cells form no trichocysts [39], so they display empty trichocyst docking sites [40].

There were different reasons to include these mutants in our studies. Considering the differences in cell cortex structure, we wanted to see whether mutants would develop similar $[Ca^{2+}]_i$ transients in response to veratridine as the wild type. Any difference may yield important functional clues. For instance, nd9–28°C cells may show internal decondensation of trichocyst contents in response to a permeable agonist [27], as we found. The tl cells may show much more pronounced $[Ca^{2+}]_i$ transients which may much more rapidly spread towards the cell interior via unoccupied trichocyst docking sites, and this is in fact what we observed. All strains analyzed contain the vast alveolar sacs system closely attached to the cell membrane, except at the origins of cilia and at docking sites of trichocysts [38]. Could veratridine mobilize Ca^{2+} from these stores in all these strains and how may this be related to Ca_o^{2+} influx? Another question we briefly addressed is the possible consequence of mutated, nonfunctional voltage-dependent Ca channels in cilia of another mutant, d4-500r ("pawn"), [20, 44]. Finally, nonsecretory mutants, nd9 and tl, were used also for technical reasons, since these cells, in contrast to 7S cells, are not vigorously dislocated during quasi-explosive trichocyst expulsion. Therefore, these strains, though mobile, are much more easily and reliably amenable to 2λ fluorochrome analysis of calibrated $[Ca^{2+}]_i$ transients, while 7S cells can be preferably used for semiquantitative, but fast, 1λ analysis on a subsecond time scale [14, 26, 27].

In our previous work with veratridine we combined quenched-flow and freeze-fracture to analyze quantitatively exocytosis by ultrastructural changes occurring at performed exocytosis sites (typical of trichocyst docking sites in *Paramecium* cells) during membrane fusion, resealing and endocytosis [36]. *Paramecium* has no voltage-dependent Na channels [32, 41] and veratridine stimulated trichocyst exocytosis is independent of Na_o^+. No immediate trichocyst secretion occurred when $[Ca^{2+}]_o$ was adjusted close to intracellular resting levels ($[Ca^{2+}]_i^{rest}$ = 50 − 100 nM, as determined for the different strains in refs. [26, 27]), e.g., to 30 nM, or when $[Ca^{2+}]_o$ was increased to unusually high, though nontoxic levels of 10 mM [36]. Previously we had no explanation for the latter quite unexpected result. Alternatively, we did not know whether Ca^{2+} may be released from cortical stores, while trichocyst expulsion cannot be seen in the absence of $Ca^{2+}{}_o$. Interestingly, with high $[Ca^{2+}]_o$ we see that $[Ca^{2+}]_i$ transients generated by veratridine are reduced and delayed.

In the current work we show that dependence of veratridine-mediated $[Ca^{2+}]_i$ transients on $[Ca^{2+}]_o$ may have two origins. (i) At low $[Ca^{2+}]_o$ (~30 nM), cortical $[Ca^{2+}]_i$ transients may develop by mobilization from alveolar sacs. (ii) At "medium" $[Ca^{2+}]_o$ (~50 μM, normally present in cultures, or up to 1 mM), additional Ca^{2+} influx is a significant component. In this case, the channel activation effects of veratridine may prevail, while (iii) at high $[Ca^{2+}]_o$ (10 mM) the membrane stabilizing effect of Ca^{2+} overrides the labilizing/activating of veratridine. An intermediate concentration obtained by diluting $[Ca^{2+}]_o$ = 10 mM to a final value of 1 mM during stimulation with a 10-fold excess of veratridine also served to rule out toxic effects of high $[Ca^{2+}]_o$. In addition, vitality was tested by dye exclusion or by monitoring the response to multiple veratridine applications. Channels actually activated by veratridine may unspecifically carry Ca, as we tentatively show by Mn^{2+}-quenched Fura-2 fluorescence [9, 16] and we try to pinpoint more clearly candidates.

Our findings may have some bearing also on the analysis of some other cells, to which veratridine is frequently used as a cell membrane channel agonist.

Materials and Methods

Cell Cultures

Paramecium tetraurelia cells were grown, monoxenically in a medium inoculated with *Enterobacter aerogenes*, in dried lettuce medium ($[Ca^{2+}]_o$ adjusted to 50 μM and $[Na^+]_o$ to 0.4 mM, [33]). Wild-type cells (strain 7S), a trichocyst-free strain "trichless" (tl) [39], and a "pawn" mutant (d4-500r) devoid of ciliary voltage dependent Ca channels [20, 44] but with normal secretory capacity were all grown at 25°C, the nondischarge mutant nd9 [3, 4, 30, 40] was grown at 28°C. All were used at early stationary phase.

Chemicals and Solutions

All fluorochromes, calcein and BAPTA were purchased from Molecular Probes (Eugene, OR). Veratridine (Sigma, Deisenhofen, Germany) was dissolved as a 25 mM stock solution in 0.025 N HCl titrated with KOH to pH 7.3.

Cell Stimulation and Microfluorometric $[Ca^{2+}]_i$ Transient Measurements

The anterior or posterior cell pole, respectively, was aligned in front of the opening of a capillary (inner diameter ~2 μm) containing the trigger

solution, with the use of a home-made turnable slide-holder. Ca^{2+} concentrations in the medium, $[Ca^{2+}]_o$, were adjusted as previously described [14] and additionally measured in parallel controls, by occasional extracellular Fura Red addition. Veratridine (in absence of Fura Red, but with defined Ca^{2+} content, as indicated in figure and table legends) was applied locally at a distance of ~10 μm from the cell, resulting in a trigger concentration of ~1 mM. In some experiments cells were incubated with $[Ca^{2+}]_o$ = 10 mM, and this was either kept at this level or diluted to 1 mM, depending on whether the trigger solution added in 10-fold excess was supplemented with Ca^{2+}. $[Ca^{2+}]_o$ = 10 mM can cause a transient $[Ca^{2+}]_i$ increase, though no exocytosis [14]. Therefore, increments were referred to $[Ca^{2+}]_i^{rest}$ at the usual $[Ca^{2+}]_o$ = 50 μM.

To chelate $[Ca^{2+}]_o$ to ~30 nM, i.e., slightly below resting levels (50–100 nM), we added 4.5 mM EGTA to the extracellular medium, as in ref. [26]. Since $[Ca^{2+}]_i$ can decrease with time, when Ca_o^{2+} is removed [12], the fast Ca^{2+} chelator BAPTA (1 mM final concentration) was eventually added to the veratridine solution. In some controls, vehicle only was applied. In other controls veratridine was applied to cells loaded with calcein to document membrane integrity [48].

$[Ca^{2+}]_i$ transients were evaluated either conventionally in the dual wavelength mode, or by fast confocal laser scanning microscopy (CLSM) in the single wavelength mode (*see* below as well as figure and table legends). In detail, all fluorochromes were dissolved in 10 mM Tris-HCl buffer pH 7.2 and microinjected to a final concentration of 50 μM (Fura Red) or 100 μM (Fluo-3, Fura-2, calcein), whereby homogenous intracellular distribution (except for closed compartments, like vacuoles and trichocysts) became visible, before $[Ca^{2+}]_i$ changes were evaluated as described previously [26]. Veratridine-induced $[Ca^{2+}]_i$ transients were conventionally analyzed with the double excitation (440/490 nm)/single emission (≥590 nm) fluorochrome Fura Red. Cell regions analyzed were either anterior or posterior, peripheral or central, respectively. As shown in the enclosed color image, defined cortical or more central cytoplasmic areas of similar size, close to or at ~30 μm distance from the cell border, respectively (boxes in Fig. 1), were evaluated. Mn^{2+}-quench of Fura-2 (λ_{ex} = 360/380 nm/λ_{em} ≥ 510 nm) was used to demonstrate veratridine-stimulated Mn^{2+} entry by unspecific Me^{2+} conducting channels [9, 16]. Confocal analysis with Fluo-3 injected cells was carried out at video rate in an Odyssey XL, Noran Instruments (Middleton, WI, and Bruchsal, Germany), λ_{ex} = 488 nm/λ_{em} ≥ 515 nm as previously described [14]. Calcein was analyzed by CLSM with the same filter set.

Exocytotic response was classified as follows. In 7S cells, veratridine-induced exocytotic response (membrane fusion and trichocyst secretory contents release by stretching ["decondensation"]) and $[Ca^{2+}]_i$ transients were correlated in time by confocal time series with alternating fluorescence and transmitted light pictures as previously described [14]. In nd9–28°C cells, veratridine-induced $[Ca^{2+}]_i$ transients were paralleled by internal trichocyst decondensation since these cells are incapable of membrane fusion, just as described for caffeine treatment [27]. The amount of veratridine-stimulated exocytosis (in 7S) or "internal decondensation" (in nd9) was classified in three categories (Tables 1, 3), namely "−, +, ++" indicating no, weak-to-medium and strong local response, respectively, upon local veratridine application.

Results

Figures 1–3 inform about $[Ca^{2+}]_i^{rest}$ and $[Ca^{2+}]_i$ transients occurring during veratridine stimulated exocytosis. Values of $[Ca^{2+}]_i^{rest}$ for the different strains are between ~50 and 100 nM, thus closely resembling values previously reported [26, 27]. Fura Red false color images can easily be obtained with tl and nd9–28°C cells (Fig. 1, middle and bottom), to be combined with calibration as previously specified [26], since these cells are not dislocated by exocytosis, which in 7S cells is so vigorous that fast CLSM/1λ analysis is advised. Since $[Ca^{2+}]_i^{rest}$ is quite similar in these strains, images obtained with Fluo-3 injected 7S cells by 1λ/CLSM analysis could be adjusted in Fig. 1 (top) to those obtained with Fura Red 2λ recordings with the other two strains analyzed. As previously described [14], high $[Ca^{2+}]_o$ values (10 mM) *per se* produce increased $[Ca^{2+}]_i^{rest}$ levels (though without ensuing exocytosis in 7S cells), and the data achieved under such conditions were also normalized to usual basal $[Ca^{2+}]_i$ levels, to visualize more clearly the increment actually produced by local veratridine stimulation. Key data derived from Figs. 2 and 3 are summarized in Tables 1 and 2.

In 7S cells, at $[Ca^{2+}]_o$ = 30 nM, veratridine causes only a rather slight cortical $[Ca^{2+}]_i$ transient which is much more pronounced at $[Ca^{2+}]_o$ = 50 μM and even more at $[Ca^{2+}]_o$ = 1 mM (by dilution of $[Ca^{2+}]_o$ = 10 mM in preincubation medium during veratridine application, as described in Materials and Methods). Most importantly, if high $[Ca^{2+}]_o$ is maintained, by adding 10 mM Ca^{2+} to the veratridine solution, the veratridine induced $[Ca^{2+}]_i$ transient is considerably delayed and reduced in amplitude (Fig. 2), while exocytosis is strongly inhibited under these conditions (Table 1), just as in our previous freeze-fracture studies [36].

Surprisingly, nd9–28°C and tl cells revealed a pronounced cortical $[Ca^{2+}]_i$ transient (Fig. 3) not only at $[Ca^{2+}]_o$ = 50 μM, but also at 30 nM, thus strongly suggesting mobilization from cortical pools, while such evidence was much less pronounced with 7S cells (Fig. 2). Spillover into central cell regions is most pronounced in tl cells, where it may be facilitated by unoccupied docking sites. This is most striking in tl cells triggered in presence of $[Ca^{2+}]_o$ = 1 mM (again by dilution during veratridine application), thus strictly indicating superposition of store mobilization by $Ca^{2+}{}_o$ influx.

Upon veratridine stimulation, cortical $[Ca^{2+}]_i$ increase can be seen within 1 to 2 sec (i.e., the time required for filter changes) in tl and nd9–28°C cells, or over slightly longer time periods in 7S and d4-500r cells (Figs. 2, 3, Tables 1, 2). In all cases, the veratridine induced $[Ca^{2+}]_i$ signal attenuates, as it sweeps, with some delay, towards the interior of the cell (Figs. 1–3).

In pilot experiments with $[Ca^{2+}]_o$ = 50 μM, d4-500r cells showed a similar reaction to veratridine as 7S cells (Fig. 2 bottom). This is comparable to data from the Cohen group [24].

Data from Figs. 1–3 can be summarized as follows. (i) Veratridine can mobilize cortical Ca pools. (ii) This may be superimposed by Ca^{2+} influx which then augments cortical $[Ca^{2+}]_i$ transients. (iii) High though not toxic $[Ca^{2+}]_o$ = 10 mM in the trigger solution inhibits

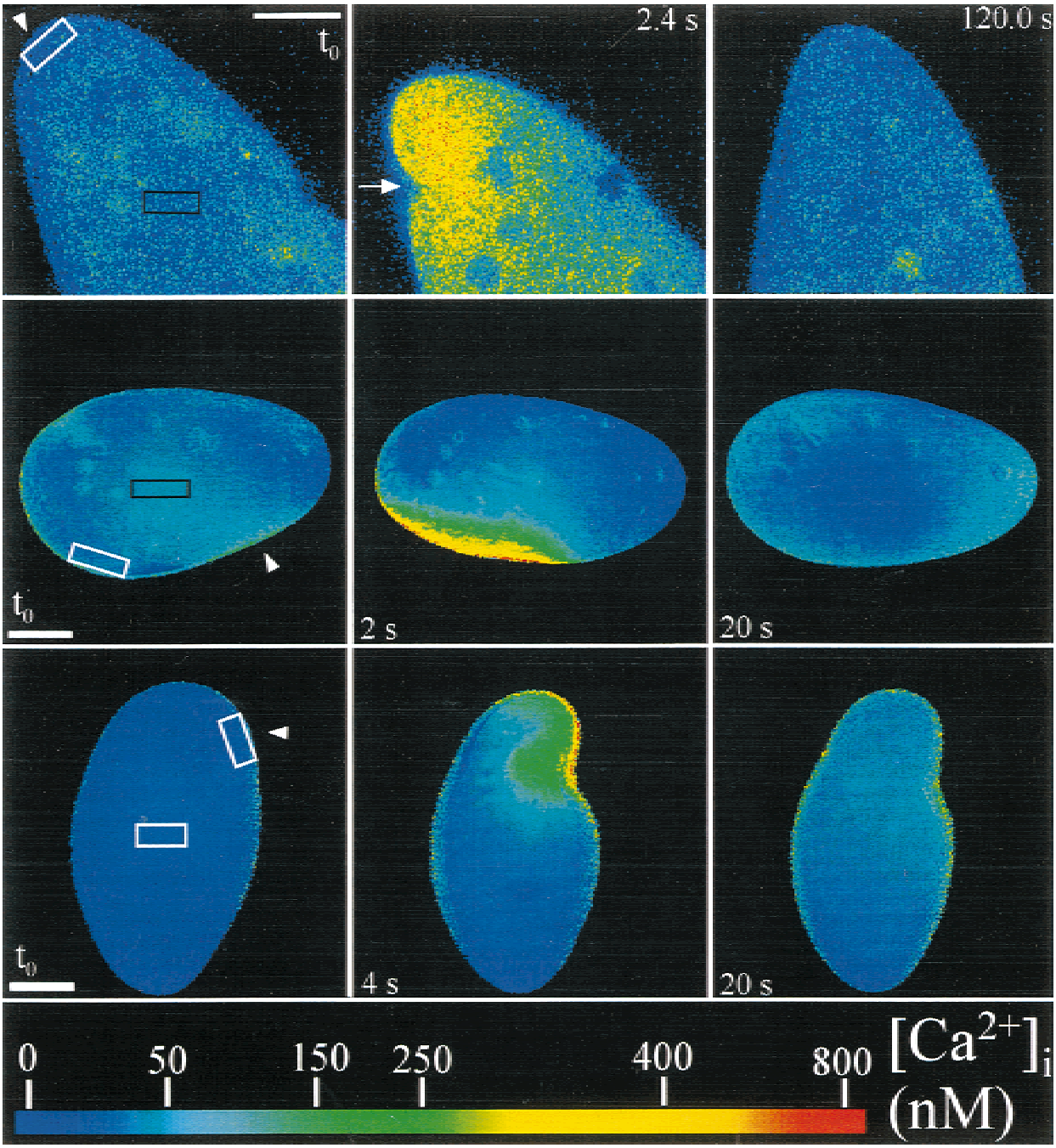

Fig. 1. False color representation of veratridine induced $[Ca^{2+}]_i$ transients at $[Ca^{2+}]_o$ = 30 nM, indicating mobilization of cortical pools. 7S (top) loaded with Fluo-3, tl (middle) and nd9-28°C cells (bottom) loaded with Fura Red and stimulated locally with veratridine (arrowheads). False color evaluation, also for Fluo-3 injected 7S, as described in the text. Note restricted cortical $[Ca^{2+}]_i$ increase accompanied by cell contraction and exocytosis (visible particularly in transmitted light images, not shown) in the wild-type 7S (region marked by arrow) and occasionally by local cell contraction and a restricted amount of trichocyst exocytosis in 7S cells. Squares indicate regions evaluated quantitatively in the figures and tables shown. Bars = 20 μm.

cortical $[Ca^{2+}]_i$ responses. (iv) With $[Ca^{2+}]_o$ = 1 mM during veratridine application, maximal $[Ca^{2+}]_i$ transients result. This implies that preincubation in high $[Ca^{2+}]_o$ exerts no toxic effects. Finally, (v) $Ca^{2+}{}_o$ influx may occur via the somatic cell membrane, although veratridine is also reported to activate defective ciliary Ca channels in "pawn" cells [47].

Tables 1 and 2 summarize more clearly some of our

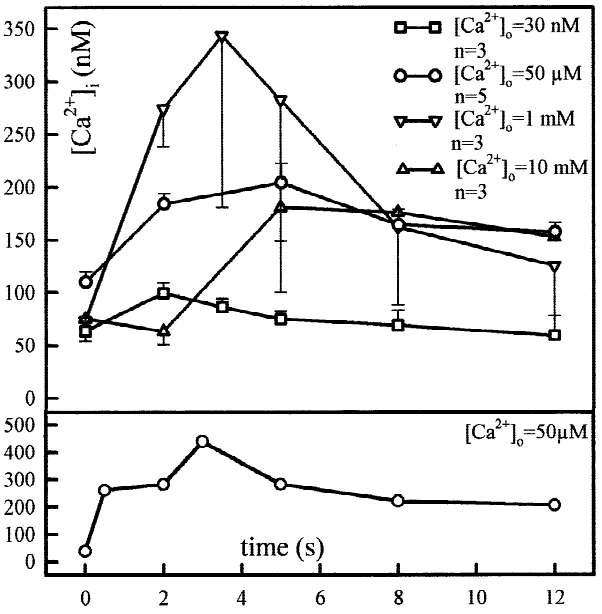

Fig. 2. Veratridine induced cortical $[Ca^{2+}]_i$ transients in 7S cells (top) and a "pawn" mutant, d4-500r (bottom), all Fura Red loaded. 7S was triggered at $[Ca^{2+}]_o$ = 30 nM, 50 µM, 1 mM (after preincubation at 10 mM and 10-fold dilution during veratridine application), or 10 mM (undiluted during veratridine application). The "pawn" cell (example representative of 3 cells evaluated) was triggered at $[Ca^{2+}]_o$ = 50 µM. Note in 7S cells immediate rise in cortical $[Ca^{2+}]_i$ in most cases, with only small, but significant cortical $[Ca^{2+}]_i$ increase at $[Ca^{2+}]_o$ = 30 nM, but considerably delayed rise in presence of $[Ca^{2+}]_o$ = 10 mM ("undiluted" during veratridine application). For further explanations, see text. Mean values ± SEM, n = number of cells analyzed.

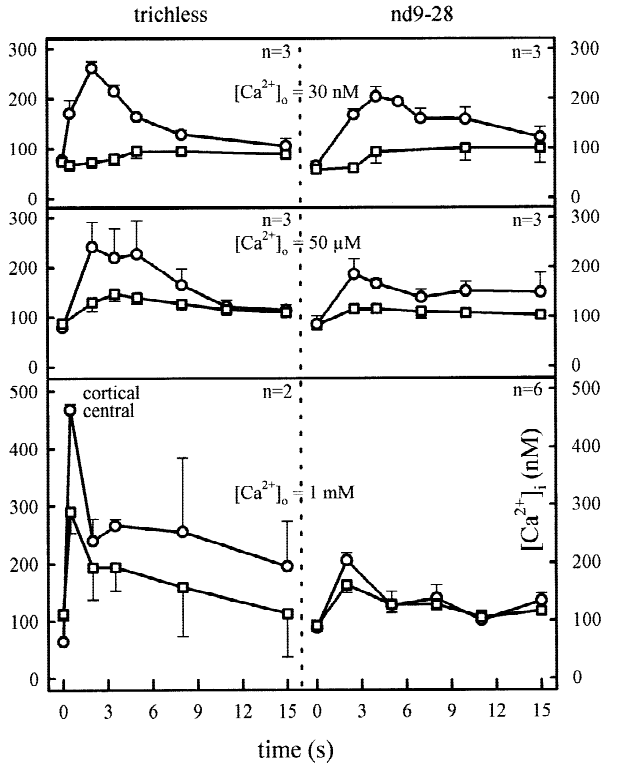

Fig. 3. Veratridine induced $[Ca^{2+}]_i$ transients in nonsecretory mutants, tl and nd9-28°C. Fura Red loaded cells were stimulated at $[Ca^{2+}]_o$ = 30 nM, 50 µM or 1 mM ($[Ca^{2+}]_o$ = 10 mM in preincubation medium, 10-fold diluted during veratridine application), respectively. Note most rapid and pronounced cortical response of tl cells. Mean values, ± SEM.

findings. (i) Not only cortical and central $[Ca^{2+}]_i$ peak values achieved by veratridine stimulation depend on $[Ca^{2+}]_o$, but also times required for increase and decay as well as recovery values achieved. (ii) Increasing $[Ca^{2+}]_o$ up to 1 mM increases the resulting $[Ca^{2+}]_i$ transients and exocytotic response. (iii) To some extent all these values vary between the different strains. As mentioned, tl may show the strongest reaction because of free diffusion pathways. Alternatively, assembly of functional docking sites in 7S cells may bind/"consume" much of free Ca_i^{2+}. One candidate is calmodulin occurring at properly assembled trichocyst exocytosis sites [25, 34]. For these reasons, the reaction of nd9–28°C may be in between tl and 7S cells. (iv) Veratridine induces trichocyst exocytosis in 7S cells (as it does in d4-500r; *data not shown*), as previously analyzed [36], while it causes internal decondensation of trichocyst contents without external release (exocytosis) in nd9–28°C cells which are incompetent for membrane fusion.

Which channels of the somatic cell membrane could conduct Ca^{2+} during veratridine stimulation? To address this question, we analyzed Mn^{2+}-induced Fura-2 quenching, as outlined in Materials and Methods. As documented in Fig. 4 with λ_{ex} = 360 nm, veratridine induces $Ca^{2+}{}_o$-insensitive fluorescence-quench only in presence of Mn^{2+}. This effect is generally attributed to involvement of unspecific Me^{2+} conductances [9, 16]. Some discontinuity, with a slight signal decay in the bottom part of Fig. 4 (without Mn^{2+}), is due to the problem that 7S cells cannot be kept totally immobile during the analysis time of 1 min.

Since in *Paramecium* some cation channels are distributed or activated unequally over the cell surface [14, 15], we analyzed, in Figs. 5 and 6, reaction of the two cell poles of 7S cells to veratridine, in presence of $[Ca^{2+}]_o$ = 50 µM or 30 nM, respectively. Though not on an absolute quantitative scale, by f/f_o ratio evaluation of rapid CLSM analysis, we could obtain data with high time resolution, as summarized in Table 3. Again, with $[Ca^{2+}]_o$ = 50 µM, veratridine produces a stronger cortical $[Ca^{2+}]_i$ transient than in presence of $[Ca^{2+}]_o$ = 30 nM, particularly in the anterior cell pole, though rates of $[Ca^{2+}]_i$ increase are not significantly different. Most remarkably, exocytotic response is also considerably stronger and faster in the anterior cell pole (Table 3) where some of the established cation channels are known to be concentrated [32, 41], as discussed below. Recovery rates are quite different in the two cell regions.

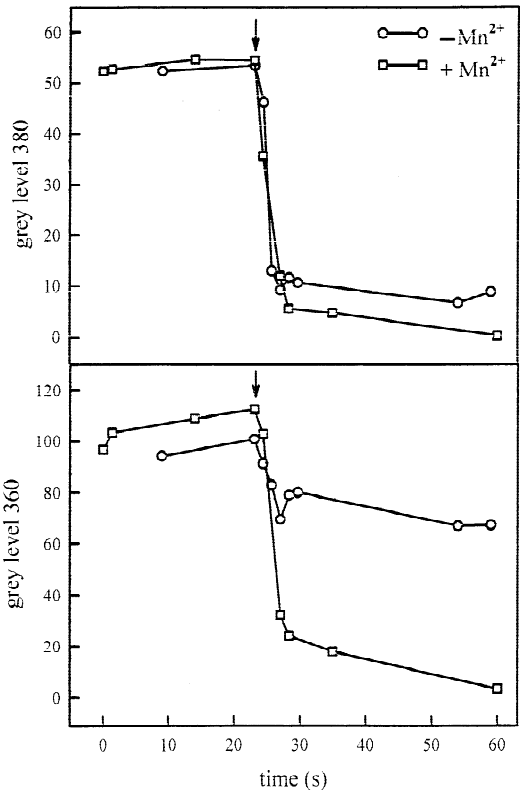

Fig. 4. Veratridine activated unspecific Me^{2+} influx shown by Mn^{2+}-quench of Fura-2 in 7S cells. After loading with Fura-2, a cell was locally triggered at its anterior pole with veratridine, another cell, also at the anterior end, with veratridine +1 mM Mn^{2+} ($[Ca^{2+}]_o$ = 50 μM). Fura-2 emission at λ_{ex} = 380 nm (top) declined in the cortex of both cells, independent of the presence/absence of Mn^{2+} in the trigger solution, indicating a rise in cortical $[Ca^{2+}]_i$. In contrast, Ca^{2+} insensitive emission of Fura-2 at λ_{ex} = 360 nm (bottom) declined significantly only in presence of Mn^{2+}, which entered the cell and quenched Fura-2 fluorescence. The slight change in absence of Mn^{2+} is due to unavoidable cell movement during mock application.

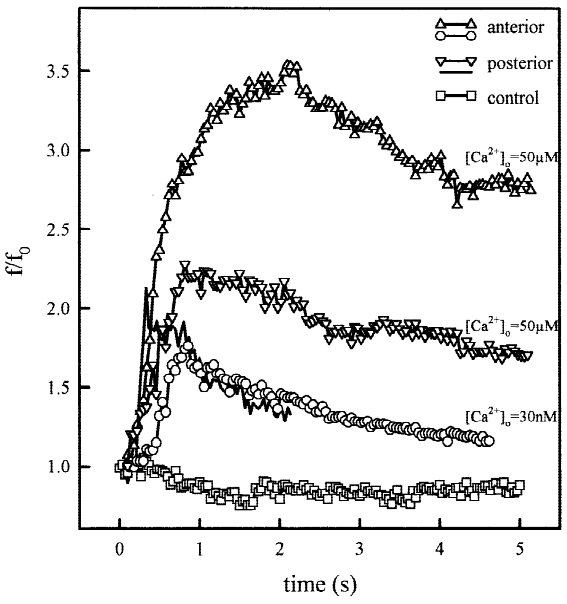

Fig. 5. Veratridine induced rise of cortical $[Ca^{2+}]_i$ at the anterior cell pole exceeds that at the posterior pole. Typical experiment with Fluo-3 loaded 7S cells locally stimulated with veratridine at their anterior or posterior end, respectively, in presence of $[Ca^{2+}]_o$ = 50 μM or 30 nM, respectively. Changes in $[Ca^{2+}]_i$ were followed in the cortical region by CLSM during 5 sec with 33 frames/sec. The amplitude of the posterior cortical $[Ca^{2+}]_i$ rise was quite similar with both $[Ca^{2+}]_o$ situations, whereas $[Ca^{2+}]_i$ increase is selectively strong at the anterior part of the cell at $[Ca^{2+}]_o$ = 50 μM, thus indicating that Ca^{2+} influx predominates in this region. For statistics, *see* Fig. 6.

Finally we document, in Fig. 7, that $[Ca^{2+}]_i$ responses to veratridine are concentration-dependent and reversible, thus again excluding toxicity. With increasing stimulation, increasing $[Ca^{2+}]_i$ responses and slightly delayed exocytosis can be achieved. In some experiments, conducted with calcein-loaded cells, we document absence of cytotoxic effects since this small marker (621 Da) does not leak under our experimental conditions (*data not shown*).

Discussion

Just like in some other cell types [2, 8, 21, 42], including neuronal systems [1, 7, 12, 13, 17, 31, 51], veratridine induces exocytosis in *Paramecium* cells [15, 24, 29, 36]. Depending on the cell type analyzed, mechanisms involved in veratridine activation may range from depolarization by activation of Na channels to Na^+_o-independent mechanisms. Only the latter can be assumed for *Paramecium* [15, 36] since these cells have no voltage-dependent Na channel [32, 41].

Which might then be the common denominator for the stimulatory effect of veratridine? Several aspects can be discussed that are only in part related to the Na channel agonist function commonly attributed to this alkaloid.

First, veratridine may act not only from the outside, but it has been shown to activate some cells, e.g., via Na channels also from inside [19, 22]. At pH 7.3, as used here for extracellular application, veratridine is lipophilic and thus can "see" targets in the cell membrane, while it also enters cells [8, 22]. The cytosolic pH of *Paramecium* is unexpectedly low, i.e., 6.6, as recently reported [11]. Protonation fully activates veratridine [22] and, thus, can explain some of the effects we see in *Paramecium*, for instance internal trichocyst decondensation, as discussed below. Paradoxically this can also explain why we achieved no exocytosis activation in 7S cells after microinjection of veratridine [36], since this was also performed in strictly buffered solution pH 7.3. In conclusion, permeation into/through membranes due to

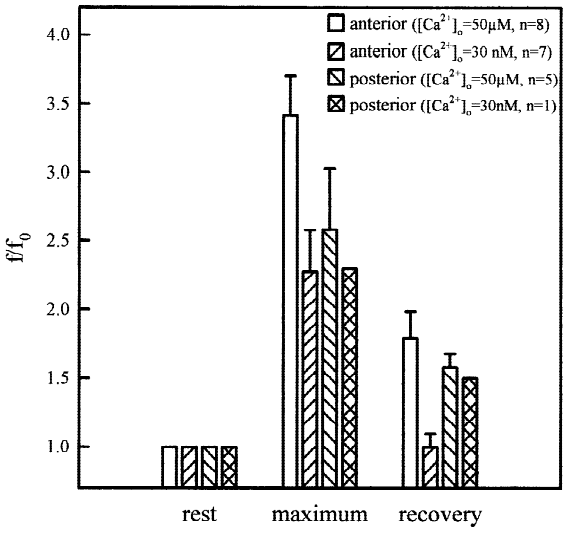

Fig. 6. Amplitude of cortical $[Ca^{2+}]_i$ in the anterior cell pole exceeds that in the posterior pole at $[Ca^{2+}]_o$ = 50 μM, but not at 30 nM. Fluo-3 loaded 7S cells were locally triggered, in presence of $[Ca^{2+}]_o$ = 50 μM or 30 nM, as indicated. Presented are cortical $[Ca^{2+}]_i$ amplidutes at 1–2 sec and at ≥10 sec, respectively, after veratridine application. Highest amplitudes occurred at anterior sites with $[Ca^{2+}]_o$ = 50 μM, thus indicating preferential anterior Ca^{2+} influx. Mean values ± SEM, *n* = number of cells analyzed.

lipid solubility [8] is highest in nonprotonated form, while protonation entails activation [22].

Second, veratridine increases lipid bilayer fluidity [7, 42], with the likely effect that different cation channels or exchangers can achieve higher open probability [8]. In some systems activation of Na channels may be the primary step [1, 7, 22, 52] entailing other steps to follow [12, 51, 52].

Third, since we observe cortical $[Ca^{2+}]_i$ transients also with $[Ca^{2+}]_o < [Ca^{2+}]_i^{rest}$, we conclude that veratridine can also activate Ca channels of cortical stores, notably alveolar sacs [49], from where $[Ca^{2+}]_i$ transients most likely take their origin. The amount released by cortical store activation is sufficient to give a remarkable signal in the present study.

Fourth, increased $[Ca^{2+}]_i$ signal in presence of $[Ca^{2+}]_o$ = 50 μM or 1 mM, respectively, indicates $Ca^{2+}{}_o$ influx in response to veratridine, in agreement with $^{45}Ca^{2+}$ flux measurements [24].

Despite the different modes of action to be assumed for the different agonists which can stimulate trichocyst exocytosis in *Paramecium* cells, $[Ca^{2+}]_i$ responses to veratridine are, with some respect, similar to those obtained with the other agonists, i.e., AED or caffeine [26, 27]. The $[Ca^{2+}]_i$ reaction is most rapid with AED [14, 37], while $[Ca^{2+}]_i$ increase is slower with caffeine [27] or with veratridine (this paper), respectively, as analyzed by rapid CLSM. Similar $[Ca^{2+}]_i$ increases were obtained with the nonpermeable secretagogue, AED, at 10^{-5} M

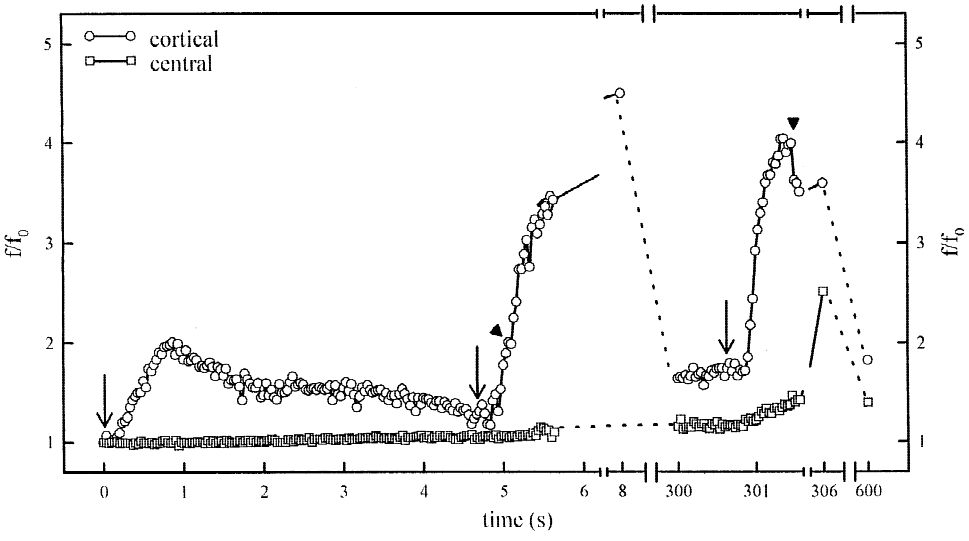

Fig. 7. Dependence of $[Ca^{2+}]_i$ response on veratridine concentration and of exocytotic response on cortical $[Ca^{2+}]_i$ rise, shown by multiple veratridine application in different concentrations to Fluo-3 loaded 7S cells in presence of $[Ca^{2+}]_o$ = 50 μM. The anterior cell end was 3times stimulated with veratridine (arrows). The first trigger was suboptimal (<1 mM veratridine due to increased distance of application pipette), evoking a 2-fold cortical signal increase but no exocytosis. The second and third trigger (≥1 mM veratridine) were applied to the same cell region 4.7 sec and 300.8 sec, respectively, after the first trigger. Both evoked a ≥4fold $[Ca^{2+}]_i$ rise in the cortex and, with a delay of 0.4 or 0.8 sec, respectively, trichocyst exocytosis (arrowheads). Central $[Ca^{2+}]_i$ increased only after the third trigger.

Table 1. Veratridine evoked $[Ca^{2+}]_i$ transients in Fura Red loaded wild-type (7S) and mutant cells at $[Ca^{2+}]_o$ = 30 nM, 50 μM, 1 mM (by dilution of 10 mM during veratridine application) and 10 mM final concentration

Strain	*n*	$[Ca^{2+}]_o$ (M)	Cortical $[Ca^{2+}]_i$			Central $[Ca^{2+}]_i$			Trichocyst reaction	
			Rest (nM)	max. (nM)	rec. (nM)	Rest (nM)	max. (nM)	Rec. (nM)	Membrane fusion	Decondensation
7S	3		65 ± 13	100 ± 10	72 ± 18	63 ± 11	62 ± 12	66 ± 22	+	+
nd9–28°C	3	3×10^{-8}	65 ± 9	204 ± 19	113 ± 22	57 ± 2	100 ± 25	89 ± 23	−	+
tl	3		77 ± 6	262 ± 13	97 ± 9	74 ± 4	95 ± 15	76 ± 11	−	−
7S	5		109 ± 6	204 ± 19	153 ± 12	109 ± 6	154 ± 9	144 ± 8	++	++
nd9–28°C	3	5×10^{-5}	85 ± 16	186 ± 31	149 ± 38	83 ± 8	116 ± 10	103 ± 6	−	+
tl	3		79 ± 2	241 ± 50	111 ± 7	87 ± 5	146 ± 14	102 ± 5	−	+
7S	3		74 ± 12	343 ± 163	124 ± 19	104 ± 7	249 ± 69	203 ± 18	++	++
nd9–28°C	6	10^{-3}	87 ± 14	204 ± 13	130 ± 26	91 ± 10	162 ± 14	110 ± 14	−	+
tl	2		64 ± 14	468 ± 10	195 ± 78	113 ± 7	290 ± 37	113 ± 75	−	−
7S	3	10^{-2}	75 ± 10	181 ± 81	152 ± 4	−	−	−	−	−

Cortical and central $[Ca^{2+}]_i$ values before stimulation ("rest"), at maximal response time ("max" at t_{max}) and 12 to 15 sec recovery ("rec") after local veratridine stimulation are indicated. Cortical $[Ca^{2+}]_i$ signals are accompanied by exocytosis in 7S (membrane fusion and contents decondensation during release), or by "internal trichocyst decondensation" in nd9-28°C cells; for evaluation of exocytotic response, *see* Materials and Methods. Mean ± SEM, *n* = number of cells analyzed.

concentration, also at $[Ca^{2+}]_o$ = 50 μM, causing maximal cortical $[Ca^{2+}]_i$ increases by a factor of ~2.9, 5.7 or 6 in 7S, nd9–28°C or tl cells, respectively. Caffeine has to enter the cell to mobilize stores, as previously discussed [27]. Concomittantly, with caffeine or veratridine, exocytosis procedes considerably more slowly than with AED [28] and both agents produce "internal trichocyst decondensation," as defined above, in nd9–28°C cells — quite in contrast to AED. This effect would be compatible with labilization of trichocyst membranes, thus allowing access of Ca^{2+} to secretory contents as cortical $[Ca^{2+}]_i$ rises to submicromolar concentrations required for "decondensation" [5, 23]. This would imply that veratridine (of caffeine) may activate so far unknown channel or transporter systems in the membranes of trichocysts whose contents are poor in Ca, but rich in Na [45].

There remains, however, a striking difference between the different agonists for trichocyst exocytosis. Only with veratridine, the stimulation of trichocyst exocytosis (analyzed in detail previously by Plattner et al. [36]) and the effect on $[Ca^{2+}]_i$ increase (this paper) is reduced with $[Ca^{2+}]_o$ = 10 mM (a concentration well tolerated by these cells). This effect remained unexplained until now, particularly since we had shown the opposite effect with AED [35] where increasing $[Ca^{2+}]_o$ to 10 mM strongly accelerates all steps of the exo-endocytotic cycle in *Paramecium.* In an experiment where veratridine was applied at $[Ca^{2+}]_o$ = 10 mM (Fig. 2), we show that, despite the steeper Ca^{2+} gradient across the cell membrane, the $[Ca^{2+}]_i$ transient is delayed and initially reduced in size (e.g., when compared to $[Ca^{2+}]_o$ = 50 μM or 1 mM, respectively, in Fig. 2) and exocytosis is inhibited (Tables 1, 2). (Inhibition of veratridine triggered trichocyst exocytosis by $[Ca^{2+}]_o$ = 5 mM was previously observed also by Kerboeuf and Cohen [24]). How can this be reconciled? We tentatively attribute this effect to the long estabished membrane stabilizing effect of Ca^{2+} [18], while at lower $[Ca^{2+}]_o$, the established labilizing effect of veratridine may cause channel activation [7, 42]. Similarly, in chromaffin cells, high $[Ca^{2+}]_o$ entails reduced veratridine-induced $[Ca^{2+}]_i$ increase [31] and catecholamine release [10, 12]. Alternatively, other membrane stabilizing agents, like quinidine, can abolish veratridine effects [50]. In addition, veratridine can bind Ca^{2+} so that it cannot enter the cell sufficiently to activate its targets. On the other side of the $[Ca^{2+}]_o$ scale, 30 nM does not allow signal amplification by Ca^{2+}-influx and thus, reduces the cortical $[Ca^{2+}]_i$ signal and exocytotic response (Tables 1, 2), when immediate membrane fusion is strongly inhibited according to previous quenched-flow/freeze-fracture analyses executed 80 msec after stimulation [36].

In addition to activation of intracellular Ca^{2+} release channels, probably located in alveolar sacs, which cell membrane channels may be activated by veratridine, i.e.,

Table 2. Veratridine-evoked $[Ca^{2+}]_i$ increments following veratridine stimulation

Strain	*n*	$[Ca^{2+}]_o$ (M)	Cortical $[Ca^{2+}]_i$ increment			Central $[Ca^{2+}]_i$ increment		
			(nM) at max.	t_{max}(s)	(nM) at rec.	(nM) at max.	t_{max}(s)	(nM) at rec.
7S	3		35	2	7	0	8	3
nd9–28°C	3	3×10^{-8}	139	4	48	43	10	32
tl	3		185	2	20	21	5	2
7S	5		95	5	44	45	5	35
nd9–28°C	3	5×10^{-5}	101	3	64	33	4	20
tl	3		162	2	32	59	4	15
7S	3		269	4	50	145	5	99
nd9–28°C	6	10^{-3}	117	2	43	71	2	19
tl	2		403	1	130	177	1	0
7S	3	10^{-2}	106	5	77	–	–	–

Represented here is the difference between $[Ca^{2+}]_i$ values at maximal response ("max" at time t_{max}) or after recovery ("rec", 12 to 15 sec), respectively, and baseline values before stimulation. Data obtained at different $[Ca^{2+}]_o$, derived from Table 1. Unless indicated otherwise, $n = 5$. For evaluation of exocytotic response, *see* Materials and Methods.

which channel activities could contribute to trichocyst exocytosis?

First, ciliary voltage dependent Ca channels are unlikely to be involved in generating a normal cortical $[Ca^{2+}]_i$ signal and exocytotic response. We conclude this from different observations. (i) Cilia and trichocyst release sites are separated by ~1 μm and mutual activation is not the rule. (ii) Activation of voltage dependent ciliary Ca channels by depolarization does not provoke trichcoyst exocytosis (*data not shown*). (iii) Veratridine causes a graded effect over the entire cell surface, with $[Ca^{2+}]_i$ and exocytotic response deminishing from the anterior to the posterior cell pole (Table 3), while such differentiation is unknown to us from cilia (though it may exist). (iv) Finally we achieved normal $[Ca^{2+}]_i$ transients and exocytosis with "pawn" cells, though their defective ciliary Ca channels may be activated by veratridine, as suggested in refs. [24, 47].

Second, as outlined above, the Mn^{2+} quenched Fura-2 fluorescence we see suggests activation of some unspecific cation conductances [9, 16]. Third, some $[Ca^{2+}]_i$ response occurring over the entire cell surface could involve different K or Na (or Ca) channels since in *Paramecium* both types are activated by Ca^{2+}, as summarized by Preston [41]. Fourth, preponderance of both, $[Ca^{2+}]_i$ signals and exocytosis performance in anterior cell regions in response to veratridine, suggest activation of unequally distributed somatic cation channels or unequal activation of equally distributed such channels, as discussed below. (An alternative explanation by unequal sensitivity of the exocytotic machinery to Ca^{2+} is unlikely, just because $[Ca^{2+}]_i$ transients are more pronounced anteriorly).

Which channels may be candidates? Mainly two channel types are reported which could meet these demands. (i) Nonvoltage dependent Na channels, characterized by Saimi [43], are activated by veratridine or some other exocytosis stimulating agents, like AED or caffeine, preferentially in the anterior cell region [15]. (ii) Mechanosensitive Ca channels could theoretically also be taken into account here because they are concentrated towards the anterior cell pole [32]. (iii) While we routinely exclude mechanical activation during secretion activation (not shown here; *see* Erxleben & Plattner [15]), activation of either type of cation channel or of any other unidentified type, possibly of some Ca channels still to be specified [46, 47] or via a newly discovered Na^+/Ca^{2+} exchanger in ciliates [6] would appear feasible or, at least, cannot be excluded. Can the number of candidates be restricted? We tend to include activation of unspecific Ca^{2+} conductances via Ca and/or Na channels, first, to explain stronger anterior $[Ca^{2+}]_i$ transients in response to veratridine, and, second, to explain Na^+_o-independent veratridine effects [36] considering that Na channels in *Paramecium* also carry Ca^{2+}, particularly at low $[Na^{2+}]_o$ [43]. In the present context, previous measurements of Ca^{2+}-dependent cGMP formation [47], whole cell-patch recordings of Ca^{2+}-activated currents [15] and $^{45}Ca^{2+}$ flux measurements [24] during veratridine activation are compatible with the trigger mechanism we discuss, yet the precise type of cell membrane channel carrying Ca^{2+} has to be established.

Table 3. Comparison of $[Ca^{2+}]_i$ response in anterior or posterior cortical and in central regions, respectively, of Fluo-3 loaded 7S cells

Cell pole (n)	$[Ca^{2+}]_o$ (M)	Cortical Ca^{2+}-transient			Central Ca^{2+}-transient			Exocytosis	
		Maximum f/f_0	$t_{1/2}$ (s)	Recovery f/f_0	Maximum f/f_0	$t_{1/2}$ (s)	Recovery f/f_0	Delay (s)	Amount
Anterior (7)	3×10^{-8}	2.3 ± 0.9	0.30 ± 0.17	1.0 ± 0.3	1.6 ± 0.6	1.2 ± 0.9	1.3 ± 0.7	0.84 ± 0.34	+
Posterior (1)		2.3	0.23	1.5	1.0	–	1.0	–	–
Anterior (8)	5×10^{-5}	3.4 ± 0.8	0.40 ± 0.24	1.8 ± 0.5	2.2 ± 1.0	2.9 ± 1.3	1.7 ± 1.1	0.31 ± 0.25	++
Posterior (5)		2.6 ± 1.0	0.79 ± 0.58	1.6 ± 0.2	1.6 ± 0.7	2.8 ± 0.4	1.4 ± 0.5	0.61 ± 0.93	+
Anterior	10^{-3}	not done							++
Posterior									++
Anterior	10^{-2}								–
Posterior									–

Either the anterior or the posterior cell pole, respectively, have been exposed to veratridine and evaluated at different $[Ca^{2+}]_o$. Indicated are fluorescence changes relative to values at rest ($f/f_0 = [Ca^{2+}]_i^{activated}/[Ca^{2+}]_i^{rest}$) as specified in Materials and Methods and Results, as well as half-times required for the response ($t_{1/2}$). For evaluation of exocytotic response, *see* Materials and Methods. Mean values ± SEM, n = number of cells analyzed.

Conclusions

In conclusion, veratridine is an alternative agonist for trichocyst exocytosis in *Paramecium* cells. Here veratridine may operate in a way independent from Na^+, yet its effect depends on $[Ca^{2+}]_o$. With high $[Ca^{2+}]_o$, i.e., 10 mM, membrane stabilizing effects may prevail over membrane labilizing/channel activating effects of veratridine. Channels involved mediate Ca^{2+} influx by some unspecific cation conductances — an effect superimposed to cortical Ca store mobilization.

We thank the unknown reviewer for his constructive criticism and his proposals to make our subject better understandable. We acknowledge financial support by the Deutsche Forschungsgemeinschaft, grant P178-12 to H.P.

References

1. Alkadhi, K.A., Tian, L.M. 1996. Veratridine-enhanced persistent sodium current induces bursting in CA1 pyramidal neurons. *Neurosci.* **71:**625–632
2. Barnes, S., Hille, B. 1988. Veratridine modifies open sodium channels. *J. Gen. Physiol.* **91:**421–443
3. Beisson, J., Cohen, J., Lefort-Tran, M., Pouphile, M., Rossignol, M. 1980. Control of membrane fusion in exocytosis. Physiological studies on a *Paramecium* mutant blocked in the final step of the trichocyst extrusion process. *J. Cell Biol.* **85:**213–227
4. Beisson, J., Lefort-Tran, M., Pouphile, M., Rossignol, M., Satir, B. 1976. Genetic analysis of membrane differentiation in *Paramecium*. Freeze-fracture study of the trichocyst cycle in wild-type and mutant strains. *J. Cell Biol.* **69:**126–143
5. Bilinski, M., Plattner, H., Matt, H. 1981. Secretory protein decondensation as a distinct Ca^{2+}-mediated event during the final steps of exocytosis in *Paramecium* cells. *J. Cell Biol.* **88:**179–188
6. Burlando, B., Marchi, B., Krüppel, T, Orunesu, M, Viarengo, A. Occurrence of Na^+/Ca^{2+} exchange in the ciliate *Euplotes crassus* and its role in Ca^{2+} homeostasis. *Cell Calcium* (**25:**153–160)
7. Cano-Abad, M.F., López, M.G., Hernández-Guijo, J.M., Zapater, P., Gandía, L., Sánchez-García, P., García, A.G. 1998. Effects of the neuroprotectant lubeluzole on the cytotoxic actions of veratridine, barium, ouabain and 6-hydroxydopamine in chromaffin cells. *Br. J. Pharmacol.* **124:**1187–1196
8. Catterall, W.A. 1980. Neurotoxins that act on voltage-sensitive sodium channels in excitable membranes. *Annu. Rev. Pharmacol. Toxicol.* **20:**15–43
9. Cheek, T.R., Morgan, A., O'Sullivan, A.J., Moreton, R.B., Berridge, M.J., Burgoyne, R.D. 1993. Spatial localization of agonist-induced Ca^{2+} entry in bovine adrenal chromaffin cells. Different patterns induced by histamine and angiotensin II, and relationship to catecholamine release. *J. Cell Sci.* **105:**913–921
10. Conceicao, I.M., Lebrun, I., Cano-Abad, M., Gandía, L., Hernández-Guijo, J.M., López, M.G., Villarroya, M., Jurkiewicz, A., García, A.G. 1998. Synergism between toxin-γ from brazilian scorpion *Tityus serrulatus* and veratridine in chromaffin cells. *Am. J. Physiol.* **274:**C1745–C1754
11. Davis, D.P., Fiekers, J.F., Van Houten, J.L. 1998. Intracellular pH and chemoresponse to NH_4^+ in *Paramecium. Cell Motil. Cytoskel.* **40:**107–118
12. Dobrev, D., Milde, A.S., Andreas, K., Ravens, U. 1998. Voltage-activated calcium channels involved in veratridine-evoked [^{3}H]dopamine release in rat striatal slices. *Neuropharmacol.* **37:**973–982
13. DoNascimento, J.L.M., Ventura, A.L.M., DeCarvalho, R.P. 1998. Veratridine- and glutamate-induced release of [^{3}H]-GABA from cultured chick retina cells: possible involvement of a GAT-1-like subtype of GABA transporter. *Brain Res.* **798:**217–222
14. Erxleben, C., Klauke, N., Flötenmeyer, M., Blanchard, M.P., Braun, C., Plattner, H. 1997. Microdomain Ca^{2+} activation during exocytosis in *Paramecium* cells. Superposition of local subplas-

malemmal calcium store activation by local Ca^{2+} influx. *J. Cell Biol.* **136:**597–607
15. Erxleben, C., Plattner, H. 1994. Ca^{2+} release from subplasmalemmal stores as a primary event during exocytosis in *Paramecium* cells. *J. Cell Biol.* **127:**935–945
16. Fasolato, C., Hoth, M., Matthews, G., Penner, R. 1993. Ca^{2+} and Mn^{2+} influx through receptor-mediated activation of nonspecific cation channels in mast cells. *Proc. Natl. Acad. Sci. USA* **90:**3068–3072
17. Finger, W., Martin, C. 1989. Quantal stores of excitatory transmitter in nerve-muscle synapses of crayfish evaluated from high-frequency asynchronous quantal release induced by veratridine or high concentrations of potassium. *Eur. J. Physiol.* **414:**437–442
18. Frankenhaeuser, B., Hodgkin, A.G. 1957. The action of calcium on the electric properties of squid axons. *J. Physiol.* (*Lond.*) **137:**218–244
19. Ghatpande, A.S., Sikdar, S.K. 1997. Competition for binding between veratridine and KIFMK: An open channel blocking peptide of the RIIA sodium channel. *J. Membrane Biol.* **160:**177–182
20. Haga, N., Forte, M., Saimi, Y., Kung, C. 1982. Microinjection of cytoplasm as a test of complementation in *Paramecium. J. Cell Biol.* **92:**559–564
21. Hille, B. 1992. Ionic Channels of Excitable Membranes. Second edition. Sinauer, Sunderland, MA
22. Honerjäger, P., Dugas, M., Zong, X.G. 1992. Mutually exclusive action of cationic veratridine and cevadine at an intracellular site of the cardiac sodium channel. *J. Gen. Physiol.* **99:**699–720
23. Kerboeuf, D., Cohen, J. 1990. A Ca^{2+} influx associated with exocytosis is specifically abolished in a *Paramecium* exocytotic mutant. *J. Cell Biol.* **111:**2527–2535
24. Kerboeuf, D., Cohen. J. 1996. Inhibition of trichocyst exocytosis and calcium influx in *Paramecium* by amiloride and divalent cations. *Biol. Cell* **86:**39–43
25. Kerboeuf, D., LeBerre, A., Dedieu, J.C., Cohen, J. 1993. Calmodulin is essential for assembling links necessary for exocytotic membrane fusion in *Paramecium. EMBO J.* **12:**3385–3390
26. Klauke, N., Plattner, H. 1997. Imaging of Ca^{2+} transients induced in *Paramecium* cells by a polyamine secretagogue. *J. Cell Sci.* **110:**975–983
27. Klauke, N., Plattner, H. 1998. Caffeine-induced Ca^{2+} transients and exocytosis in *Paramecium* cells. A correlated Ca^{2+} imaging and quenched-flow/freeze-fracture analysis. *J. Membrane Biol.* **161:**65–81
28. Knoll, G., Braun, C., Plattner, H. 1991. Quenched flow analysis of exocytosis in *Paramecium* cells: Time course, changes in membrane structure, and calcium requirements revealed after rapid mixing and rapid freezing of intact cells. *J. Cell Biol.* **113:**1295–1304
29. Knoll, G., Kerboeuf, D., Plattner, H. 1992. A rapid calcium influx during exocytosis in *Paramecium* cells is followed by a rise in cyclic GMP within 1 sec. *FEBS Lett.* **304:**265–268
30. Lefort-Tran, M., Aufderheide, K., Pouphile, M., Rossignol, M., Beisson, J. 1981. Control of exocytotic processes: cytological and physiological studies of trichocyst mutants in *Paramecium tetraurelia. J. Cell Biol.* **88:**301–311
31. López, M.G., Artalejo, A.R., García, A.G., Neher, E., García-Sancho, J. 1995. Veratridine-induced oscillations of cytosolic calcium and membrane potential in bovine chromaffin cells. *J. Physiol.* (*Lond.*) **482:**15–27
32. Machemer, H. 1988. Electrophysiology. *In: Paramecium.* H.D. Görtz, editor, pp. 185–215. Springer-Verlag, Berlin, Heidelberg, New York
33. Matt, H., Bilinski, M., Plattner, H. 1978. Adenosinetriphosphate, calcium and temperature requirements for the final steps of exocytosis in *Paramecium* cells. *J. Cell Sci.* **32:**67–86
34. Momayezi, M., Kersken, H., Gras, U., Vilmart-Seuwen, J., Plattner, H. 1986. Calmodulin in *Paramecium tetraurelia*: Localization from the in vivo to the ultrastructural level. *J. Histochem. Cytochem.* **34:**1621–1638
35. Plattner, H., Braun, C., Hentschel, J. 1997. Facilitation of membrane fusion during exocytosis and exocytosis-coupled endocytosis and acceleration of "ghost" detachment in *Paramecium* by extracellular calcium. A quenched-flow/freeze-fracture analysis. *J. Membrane Biol.* **158:**197–208
36. Plattner, H., Braun, C., Klauke, N., Länge, S. 1994. Veratridine triggers exocytosis in *Paramecium* cells by activating somatic Ca channels. *J. Membrane Biol.* **142:**229–240
37. Plattner, H., Knoll, G., Pape, R. 1993. Synchronization of different steps of the secretory cycle in *Paramecium tetraurelia*: trichocyst exocytosis, exocytosis-coupled endocytosis, and intracellular transport. *In:* Membrane Traffic in Protozoa. H. Plattner, editor. pp. 123–148. JAI Press, Greenwich, CT, London
38. Plattner, H., Lumpert, C.J., Knoll, G., Kissmehl, R, Höhne, B., Momayezi, M., Glas-Albrecht, R. 1991. Stimulus-secretion coupling in *Paramecium* cells. *Eur. J. Cell Biol.* **55:**3–16
39. Pollack, S. 1974. Mutations affecting the trichocysts in *Paramecium aurelia.* I. Morphology and description of the mutants. *J. Protozol.* **21:**352–362
40. Pouphile, M., Lefort-Tran, M., Plattner, H., Rossignol, M., Beisson, J. 1986. Genetic dissection of the morphogenesis of exocytosis sites in *Paramecium. Biol. Cell* **56:**151–162
41. Preston, R.R. 1990. Genetic dissection of Ca^{2+}-dependent ion channel function in *Paramecium. BioEssays* **12:**273–281
42. Røed, A. 1994. An inhibitory effect of veratridine during tetanic stimulation of the rat diaphragm. *Acta Physiol. Scand.* **150:**389–395
43. Saimi, Y. 1986. Calcium-dependent sodium currents in *Paramecium*: mutational manipulations and effects of hyper- and depolarization. *J. Membrane Biol.* **92:**227–236
44. Satow, Y., Kung, C. 1980. Membrane currents of pawn mutants of the pwA group in *Paramecium tetraurelia. J. Exp. Biol.* **84:**57–71
45. Schmitz, M., Zierold, K. 1989. X-ray microanalysis of ion changes during fast processes of cells, as exemplified by trichocyst exocytosis of *Paramecium caudatum. In*: Electron Microscopy of Subcellular Dynamics. H. Plattner, editor, pp. 325–339. CRC Press, Boca Raton, FL
46. Schultz, J.E., Guo, Y.L., Kleefeld, G., Völkel, H. 1997. Hyperpolarization and depolarization-activated Ca^{2+} currents in *Paramecium* trigger behavioral changes and cGMP formation independently. *J. Membrane Biol.* **156:**251–259
47. Schultz, J.E., Schade, U. 1989. Veratridine induces a Ca^{2+} influx, cyclic GMP formation, and backward swimming in *Paramecium tetraurelia* wild-type cells and Ca^{2+} current-deficient pawn mutant cells. *J. Membrane Biol.* **109:**251–258
48. Small, D.L., Monette, R., Buchan, A.M., Morley, P. 1997. Identification of calcium channels involved in neuronal injury in rat hippocampal slices subjected to oxygen and glucose deprivation. *Brain Res.* **753:**209–218
49. Stelly, N., Mauger, J.P., Kéryer, G., Claret, M., Adoutte, A. 1991. Cortical alveoli of *Paramecium*: A vast submembranous calcium storage compartment. *J. Cell Biol.* **113:**103–112
50. Tong, A.C.Y., Rattigan, S., Clark, M.G. 1998. Similarities between vasoconstrictor- and veratridine-stimulated metabolism in perfused rat hind limb. *Can. J. Physiol. Pharmacol.* **76:**125–132
51. Tretter, L., Adam-Vizi, V. 1998. The neuroprotective drug vinpocetine prevents veratridine-induced $[Na^+]_i$ and $[Ca^{2+}]_i$ rise in synaptosomes. *Neurorep.* **9:**1849–1853
52. Uezono, Y., Wada, A., Yanagihara, N., Kobayashi, H., Mizuki, T., Terao, T., Koda, Y., Izumi, F. 1992. Veratridine causes the Ca^{2+}-dependent increase in diacylglycerol formation and translocation of protein kinase C to membranes in cultured bovine adrenal medullary cells. *Arch. Pharmacol.* **346:**76–81